

# Simultaneous dose and dose rate optimization (SDDRO) of the FLASH effect for pencil-beam-scanning proton therapy

Hao Gao<sup>1,#</sup> | Jiulong Liu<sup>2,#</sup> | Yuting Lin<sup>1</sup> | Gregory N Gan<sup>1</sup> | Guillem Pratx<sup>3</sup> | Fen Wang<sup>1</sup> | Katja Langen<sup>4</sup> | Jeffrey D Bradley<sup>4</sup> | Ronny L Rotondo<sup>1</sup> | Harold H Li<sup>1</sup> | Ronald C Chen<sup>1</sup>

<sup>1</sup> Department of Radiation Oncology, University of Kansas Medical Center, Kansas City, Kansas, USA

<sup>2</sup> LSEC, Institute of Computational Mathematics and Scientific/Engineering Computing, Academy of Mathematics and Systems Science, Chinese Academy of Sciences, Beijing, China

<sup>3</sup> Department of Radiation Oncology, Stanford University, Stanford, California, USA

<sup>4</sup> Department of Radiation Oncology, Emory University, Atlanta, Georgia, USA

## Correspondence

Hao Gao, Department of Radiation Oncology, University of Kansas Medical Center, Kansas City, Kansas, USA.  
Email: hgao2@kumc.edu

#Co-first authors with equal contribution

## Funding information

NIH, Grant/Award Number: R37CA250921

## Abstract

**Purpose:** Compared to CONV-RT (with conventional dose rate), FLASH-RT (with ultra-high dose rate) can provide biological dose sparing for organs-at-risk (OARs) via the so-called FLASH effect, in addition to physical dose sparing. However, the FLASH effect only occurs, when both dose and dose rate meet certain minimum thresholds. This work will develop a simultaneous dose and dose rate optimization (SDDRO) method accounting for both FLASH dose and dose rate constraints during treatment planning for pencil-beam-scanning proton therapy.

**Methods:** SDDRO optimizes the FLASH effect (specific to FLASH-RT) as well as the dose distribution (similar to CONV-RT). The nonlinear dose rate constraint is linearized, and the reformulated optimization problem is efficiently solved via iterative convex relaxation powered by alternating direction method of multipliers. To resolve and quantify the generic tradeoff of FLASH-RT between FLASH and dose optimization, we propose the use of FLASH effective dose based on dose modifying factor (DMF) owing to the FLASH effect.

**Results:** FLASH-RT via transmission beams (TB) (IMPT-TB or SDDRO) and CONV-RT via Bragg peaks (BP) (IMPT-BP) were evaluated for clinical prostate, lung, head-and-neck (HN), and brain cases. Despite the use of TB, which is generally suboptimal to BP for normal tissue sparing, FLASH-RT via SDDRO considerably reduced FLASH effective dose for high-dose OAR adjacent to the target. For example, in the lung SBRT case, the max esophageal dose constraint 27 Gy was only met by SDDRO (24.8 Gy), compared to IMPT-BP (35.3 Gy) or IMPT-TB (36.6 Gy); in the brain SRS case, the brain constraint  $V_{12Gy} \leq 15\text{cc}$  was also only met by SDDRO (13.7cc), compared to IMPT-BP (43.9cc) or IMPT-TB (18.4cc). In addition, SDDRO substantially improved the FLASH coverage from IMPT-TB, e.g., an increase from 37.2% to 67.1% for lung, from 39.1% to 58.3% for prostate, from 65.4% to 82.1% for HN, from 50.8% to 73.3% for the brain.

**Conclusions:** Both FLASH dose and dose rate constraints are incorporated into SDDRO for FLASH-RT that jointly optimizes the FLASH effect and physical dose distribution. FLASH effective dose via FLASH DMF is introduced to reconcile the tradeoff between physical dose sparing and FLASH sparing, and quantify the net effective gain from CONV-RT to FLASH-RT.

## KEYWORDS

dose rate optimization, FLASH dose modifying factor, IMPT, proton therapy

## 1 | INTRODUCTION

The radiation delivered at ultra-high dose rates (FLASH radiotherapy (RT)), can reduce normal tissue toxicities, compared to the radiation of the same dose delivered at conventional dose rates (CONV-RT).<sup>1–10</sup> Such biological or biochemical sparing of normal tissues while preserving the tumor response via FLASH is often referred to as the FLASH effect. In addition to the requirement of ultra-high dose rates (e.g., 40 Gy/s), the occurrence of the FLASH effect also requires the sufficiently high dose (e.g., 8 Gy).<sup>1,11</sup>

Although the understanding of FLASH mechanisms is still under development,<sup>11–15</sup> a key for FLASH is the radiation at ultra-high dose rates. For clinical FLASH treatments, proton RT is a natural choice for its capability of delivering ultra-high dose rates to deep tumor targets.<sup>16,17</sup> The feasibility of FLASH delivery has been demonstrated on various commercially available proton systems.<sup>18–27</sup> Currently a clinical trial<sup>26</sup> and several large-animal studies (e.g., ref. 27) via proton FLASH are under investigation.

Despite the critical dependence of ultra-high dose rates to achieve the FLASH effect, existing treatment planning methods do not optimize the dose rate distribution and only optimize the dose distribution.<sup>28,29</sup> Given the importance of dose rate distribution to FLASH, we developed a new optimization method that optimizes both dose and dose rate distributions, called Simultaneous Dose and Dose Rate optimization (SDDRO).<sup>30</sup> However, in Gao et al,<sup>30</sup> the FLASH effect was assumed to depend only on the dose rate. Given that the FLASH effect also has the minimum dose threshold, this work will also incorporate the dose dependence of the FLASH effect into SDDRO, which will optimize dose and dose-rate constraints for the FLASH effect and the dose distribution at the same time. The details are provided in Section 2.1.

However, the optimization of the FLASH effect and the optimization of dose distribution pose a tradeoff in treatment planning, for two following reasons. First, for normal tissues that may qualify for the FLASH effect, while the goal of dose optimization is to minimize the dose, the satisfaction of the FLASH effect requires the dose to be at least a certain minimum threshold (e.g., 8 Gy), and therefore the FLASH optimization may have to increase the dose in order to achieve the FLASH effect. Second, regardless of the first reason, maximizing the FLASH effect and minimizing the dose to normal tissues are two competing optimization objectives that can form a planning tradeoff in the sense of multi-criteria optimization.<sup>31</sup> Note that the tradeoff between FLASH maximization and dose minimization to normal tissues is generic to FLASH, and not specific to SDDRO methods.

In light of the tradeoff between FLASH optimization and dose optimization, one needs to address: (1) Is there any gain to normal tissues via FLASH-RT? (2) If

so, what is the net change from CONV-RT to FLASH-RT? To answer these questions, we propose the use of FLASH effective dose as a post-optimization evaluation tool, which is a voxel-by-voxel product of physical dose and Dose Modifying Factor (DMF) owing to the FLASH effect, in order to quantify the effective gain via FLASH-RT. The details are provided in Section 2.3.

## 2 | METHODS AND MATERIALS

### 2.1 | FLASH optimization via SDDRO

While our previous work accounts for the minimum dose rate threshold  $\gamma_0$ , the major contribution of this work is to also include the minimum dose threshold  $d_0$  that triggers the FLASH effect. In addition, we will improve the optimization algorithm by linearizing the dose rate constraint.

To illustrate new methods in this work, we consider a simplified SDDRO problem

$$\min_x \|Ax - b\|^2 \text{ s.t. } \begin{cases} x^3 \geq x^2 g \\ \gamma \geq \gamma_0 \\ d \geq d_0 \end{cases} \quad (1)$$

In Equation (1),  $x$  represents proton spot weights to be optimized,  $b$  the weighted vector of objective constraint values,  $A$  the forward system matrix that is a linear operator mapping from  $x$  to  $b$ , and  $g$  the minimum spot weight threshold (namely minimum monitor-unit (MU) constraint). Without loss of generality, Equation (1) skips the optimization of  $g$  and consolidates dose influence matrix  $D$ , projections from the entire dose to different volumes corresponding to dose-volume constraints, and objective weighting into  $A$ , to better illustrate new SDDRO components in this work.

The constraints in Equation (1) include (1) the minimum MU constraint on the spot weight  $x$  that  $x$  is non-negative and  $x \geq g$  holds for positive  $x$ ; (2) the FLASH dose rate constraint on  $\gamma$ ; (3) the FLASH dose constraint on  $d$ . Since the FLASH effect (requiring high dose and dose rate) usually only occurs close to the treatment target, the FLASH constraints are enforced in a region of interest (ROI) in the vicinity of the target instead of everywhere. Without loss of generality, we skip the robust optimization and optimize with respect to the planning target volume (PTV), and enforce the FLASH constraint region only in ROI = PTV10mm, which is a 10 mm expansion of PTV. Note that the choice of 10 mm is empirically optimal compared to 5 mm, 20 mm, and 40 mm (see Supplementary Material of ref. 39), in terms of achieving balanced plan quality and ultrahigh-dose-rate coverage. However, the optimal choice of the margin can be case-dependent, for example, a larger

margin than 10 mm may be needed to capture the entire high-dose region for a certain target.

The physical dose  $d$  is computed by

$$d_i = \sum_{j=1}^{N_x} D_{ij} x_j, \quad i \leq N_d. \quad (2)$$

Here,  $D$  is the dose influence matrix,  $N_x$  the number of proton spots, and  $N_d$  the number of spatial voxels. Note the subtle difference between  $A$  and  $D$ :  $A$  is not the same as  $D$ , although  $A$  consists of  $D$  and also other components (projection and weighting for planning objectives).

The dose rate  $\gamma$  depends on  $x$  via dose-averaged dose rate formula (DADR)<sup>28</sup>

$$\gamma_i = \frac{1}{d_i} \sum_{j=1}^{N_x} B_{ij} x_j, \quad B_{ij} = D_{ij}^2 \frac{g_j}{t_j}. \quad (3)$$

Here,  $t$  is the delivery time of minimum MU  $g$ , and therefore  $g/t$  corresponds to the beam intensity. While  $t$  is often set to a constant,  $g$  can be energy-layer dependent.<sup>32</sup> However, for our purpose,  $D$ ,  $g$ , and  $t$  are consolidated into  $B$  in Equation (3), a single operator that denotes the computation of mean dose rate.

Since the  $x$  dependence in  $\gamma$  appears in both denominator and numerator of Equation (3), the direct dose rate constraint in Equation (1) is nonlinear with respect to  $x$ . To avoid optimization difficulty due to the nonlinearity, we introduce

$$C = B - \gamma_0 D. \quad (4)$$

and linearize the dose rate constraint in Equation (1), so that SDDRO is reformulated as

$$\begin{aligned} & \min_x \|Ax - b\|^2 \\ & \text{s.t.,} \begin{cases} x^3 \geq x^2 g \\ Cx \geq 0 \\ Dx \geq d_0 \end{cases} \end{aligned} \quad (5)$$

Note that the constraints in Equation (5) are a linear optimization problem except the minimum MU constraint. However, the minimum MU constraint can be solved with an analytical formula (Equation 10), and therefore there is no need to linearize the minimum MU constraint.

## 2.2 | Optimization algorithm

The linearized SDDRO can be conveniently solved by Alternating Direction Method of Multipliers (ADMM),<sup>33,34</sup> Here we briefly provide ADMM based solution algorithm for solving Equation (5), for which the dummy variables

$(z_1, z_2, z_3)$  are introduced corresponding to each constraint. Then the optimizer of Equation (5) is to iteratively solve the following augmented Lagrangian of Equation (5)

$$\begin{aligned} L(x, u_1, z_1, u_2, z_2, u_3, z_3) &= \|Ax - b\|^2 + \mu_1 \|x - z_1 + u_1\|_2^2 \\ &+ \mu_2 \|Cx - z_2 + u_2\|_2^2 + \mu_3 \|Dx - z_3 + u_3\|_2^2 \\ \text{s.t.,} \begin{cases} z_1^3 \geq z_1^2 g \\ z_2 \geq 0 \\ z_3 \geq d_0 \end{cases} \end{aligned} \quad (6)$$

in which  $(u_1, u_2, u_3)$  are dual variables of  $(z_1, z_2, z_3)$  and  $(\mu_1, \mu_2, \mu_3)$  are regularization parameters for each constraint.

That is, the solution of Equation (5) is obtained via the following iterations indexed by  $k$

$$\left\{ \begin{array}{l} x^{k+1} = \arg \min_x L(x, z_1^k, u_1^k, z_2^k, u_2^k, z_3^k, u_3^k) \\ z_1^{k+1} = \arg \min_{z_1} L(x^{k+1}, z_1, u_1^k, z_2^k, u_2^k, z_3^k, u_3^k) \\ \quad u_1^{k+1} = u_1^k + x^{k+1} - z_1^{k+1} \\ z_2^{k+1} = \arg \min_{z_2} L(x^{k+1}, z_1^{k+1}, u_1^{k+1}, z_2, u_2^k, z_3^k, u_3^k) \\ \quad u_2^{k+1} = u_2^k + Cx^{k+1} - z_2^{k+1} \\ z_3^{k+1} = \arg \min_{z_3} L(x^{k+1}, z_1^{k+1}, u_1^{k+1}, z_2^{k+1}, u_2^{k+1}, z_3, u_3^k) \\ \quad u_3^{k+1} = u_3^k + Dx^{k+1} - z_3^{k+1} \end{array} \right. \quad (7)$$

The  $x$ -subproblem is a differentiable least-square problem, which can be solved by

$$\begin{aligned} x^{k+1} &= (A^T A + \mu_1 + \mu_2 C^T C + \mu_3 D^T D)^{-1} \\ &\times (A^T b + \mu_1 (z_1^k - u_1^k) + \mu_2 C^T (z_2^k - u_2^k) \\ &+ \mu_3 D^T (z_3^k - u_3^k)) \end{aligned} \quad (8)$$

In the implementation, there is no need to explicitly form the entire matrix and then take its inverse, and Equation (8) can be efficiently solved via the conjugate gradient method since the matrix is symmetric positive definite.

The  $z$ -subproblems have analytical solutions, i.e.,

$$\left\{ \begin{array}{l} z_1^{k+1} = S(x^{k+1} + u_1^k, g) \\ z_2^{k+1} = \max(Cx^{k+1} + u_2^k, 0) \\ z_3^{k+1} = \max(Dx^{k+1} + u_3^k, d_0) \end{array} \right. \quad (9)$$

where

$$S(z, g) = \begin{cases} 0, & z < g/2 \\ \max(z, g), & \text{if } z \geq g/2 \end{cases}. \quad (10)$$

Note that the full version of SDDRO<sup>30</sup> will need to account for dose-volume constraints (nonconvex), and optimization of  $g$ , which can be solved by iterative convex relaxation<sup>35–39</sup> together with ADMM.

## 2.3 | FLASH effective dose via DMF

As explained in the introduction, the FLASH optimization and the dose optimization for normal tissues pose a generic tradeoff for FLASH treatment planning. Moreover, the optimization of the FLASH effect does not yet directly translate to certain dosimetric benefit. For these two reasons, we propose the use of FLASH effective dose to reconcile the tradeoff and quantify the net effective change of FLASH from CONV.

FLASH effective dose  $d_e$  is the voxel-by-voxel product of the original dose  $d$  and DMF owing to the FLASH effect, that is,

$$d_e = d \cdot DMF. \quad (11)$$

The DMF can be defined via the product of two indicator functions

$$DMF = 1 + (f - 1) \cdot 1_{\gamma \geq \gamma_0} \cdot 1_{d \geq d_0}. \quad (12)$$

That is,  $DMF = f$ , only for the voxels where both dose and dose rate FLASH constraints are met; otherwise,  $DMF = 1$ , that is, no FLASH effect. Here  $f$  is a given DMF constant from the literature, that is,  $f = 0.7$ ,<sup>16</sup> while DMF is a function to model the FLASH effect. Note that DMF is deliberately set to 1 in the tumor target, to reflect the current understanding of the FLASH effect.

Alternatively, the occurrence of the FLASH effect can be modeled as smoothly varying functions with respect to  $(\gamma_0, d_0)$  instead, e.g., by replacing step indicator functions in Equation (12) with sigmoid functions and fitting to multiple  $f$  values at different combinations of  $(\gamma_0, d_0)$ , that is,

$$DMF = 1 + (f - 1) \cdot s\left(k_1 \frac{Cx}{\gamma_0}\right) \cdot s\left(k_2 \frac{Dx - d_0}{d_0}\right), \quad (13)$$

where the sigmoid function is

$$s(x) = \frac{1}{\sqrt{1 + e^{-x}}}. \quad (14)$$

The parameters  $k_1$  and  $k_2$  in Equation (13) are to control the transition speed in  $\gamma$  and  $d$  respectively from CONV ( $DMF = 1$ ) to FLASH ( $DMF = f$ ). FLASH effective dose here will be based on Equation (13), which can model the transition from CONV to FLASH; in contrast, Equation (12) is binary without the translation.

While Equations (12–13) allow the use of voxel or organ-specific DMF,  $f$  is a constant in this work, which will be sufficient to evaluate the net effective change from CONV to FLASH. Based on a review paper on FLASH DMF,<sup>16</sup> here we set  $f = 0.7$  (i.e., the normal-tissue damage caused by 0.7 Gy from CONV is equivalent to that by 1 Gy from FLASH), with the FLASH thresholds  $\gamma_0 = 40$  Gy/s and  $d_0 = 8$  Gy. On the other hand, without loss of generality, the FLASH model Equation (13) with rapid translation from CONV to FLASH (i.e.,  $k_1 = k_2 = 100$ ) based on a single set of  $(\gamma_0, d_0, f)$  is used here, which is sufficient for this proof-of-concept study, although  $(k_1, k_2)$  can be fitted from multiple sets of  $(\gamma_0, d_0, f)$ , which do not pose an additional mathematical challenge to the proposed plan optimization via Equation (1) and the plan evaluation via Equation (13).

## 2.4 | Materials

CONV was planned with standard Bragg peaks (BP) via IMPT (“IMPT-BP”). FLASH was planned with transmission beams (TB) via IMPT (“IMPT-TB”) and SDDRO (“SDDRO”), respectively. Three methods IMPT-BP, IMPT-TB, and SDDRO were compared for lung (12 Gy  $\times$  3 fractions), prostate (12 Gy  $\times$  3 fractions), head-and-neck (HN) (15 Gy  $\times$  4 fractions), and brain (16 Gy  $\times$  1 fraction) cases. The dose-volume planning constraints for organs at risk (OAR) from HyTEC<sup>40</sup> were used for these SBRT/SRS plans. The FLASH effect was optimized for SDDRO in ROI = PTV10mm (a 10 mm expansion of PTV). All plans were normalized to have D95 = 100% to PTV. After the optimization with respect to the physical dose, FLASH effective dose was retrospectively evaluated via Equation (13) with  $\gamma_0 = 40$  Gy/s,  $d_0 = 8$  Gy,  $f = 0.7$ , and  $k_1 = k_2 = 100$  for all methods.

The dose influence matrices  $D$  were generated via MatRad<sup>41</sup> with 5 mm spot width (full width half maximum), and 3 mm lateral spacing on 3 mm<sup>3</sup> dose grid. For BP, 3 mm longitudinal spacing was used for spot energy discretization; for TB, only 229 MeV energy was used. The beam angles for CONV and FLASH were both (0°, 120°, 240°) for lung and brain, (90°, 270°) and (50°, 310°) respectively for prostate, (45°, 135°, 225°, 315°), and (0°, 45°, 90°, 135°) respectively for HN. The choice of beam angles was empirical, with the general principle to maximize angular gaps between beam angles. However, note that the range of beam angle choice for TB is effectively 180° instead of 360°, because a TB of  $\theta^\circ$  is essentially the same as TB of  $\theta^\circ + 180^\circ$ , that is, the

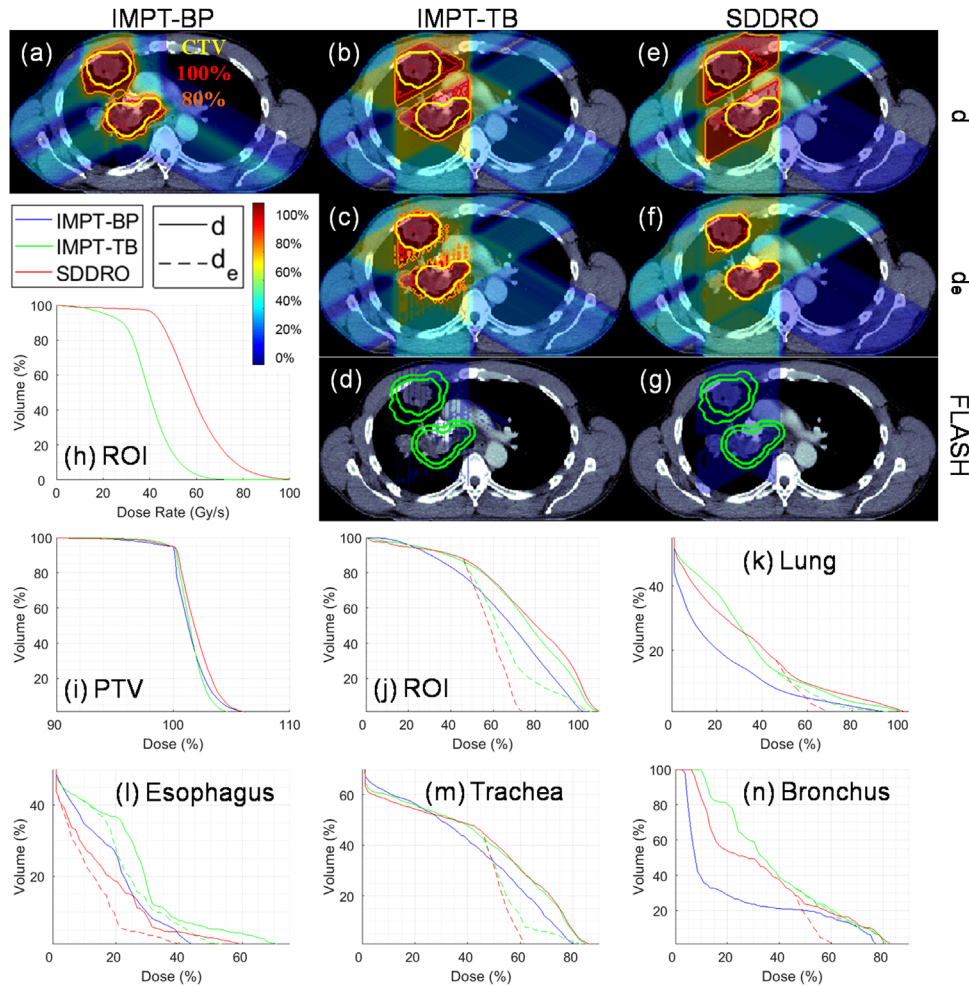


**FIGURE 1** Lung. IMPT-BP: plot of dose in (a); IMPT-TB: plots of physical dose, FLASH effective dose, and FLASH coverage in (b)-(d); SDDRO: plots of physical dose, FLASH effective dose, and FLASH coverage in (e)-(g); DRVH for ROI in (h); DVH for PTV, ROI, lung, esophagus, trachea, and bronchus in (i)-(n). The dose plot window is [0%, 110%]. 100% isodose line, 80% isodose line, and PTV are highlighted in dose plots; ROI = PTV10mm is highlighted in FLASH coverage plots, in which the blanked region is without the FLASH effect

opposing beams do not provide additional optimization degrees of freedom for TB.

In the tables, the conformal index (CI) is defined as  $V_{100}^2 / (V \times V_{100})$  ( $V_{100}$ : PTV volume receiving at least 100% of prescription dose;  $V$ : PTV volume;  $V_{100}$ : total volume receiving at least 100% of prescription dose; ideally  $CI = 1$ ); the FLASH coverage of ROI refers to the percentage of ROI volume receiving both  $\gamma \geq \gamma_0$  and  $d \geq d_0$ .

### 3 | RESULTS

The results for lung, prostate, HN, and brain are presented in Figures 1–4, respectively, for CONV (IMPT-BP) and FLASH (IMPT-TB or SDDRO). The dose parameters with respect to physical dose and FLASH effective dose are calculated and summarized in Table 1 and 2

respectively. The dose-rate coverage and FLASH coverage are summarized in Table 3.

#### 3.1 | Improving FLASH coverage via SDDRO

The FLASH coverage (i.e.,  $\gamma \geq 40 \text{ Gy/s}$  and  $d \geq 8 \text{ Gy}$ ) comparison between IMPT-TB and SDDRO for ROI = PTV10mm in Table 3 indicates SDDRO improved the FLASH coverage from IMPT-TB, i.e., an increase from 37.2% to 67.1% for lung, from 39.1% to 58.3% for prostate, from 65.4% to 82.1% for HN, and from 50.8% to 73.3% for the brain. The improved FLASH coverage via SDDRO is also confirmed through the comparison of the binary plots for FLASH coverage between IMPT-TB (Figures 1–4d) and FLASH

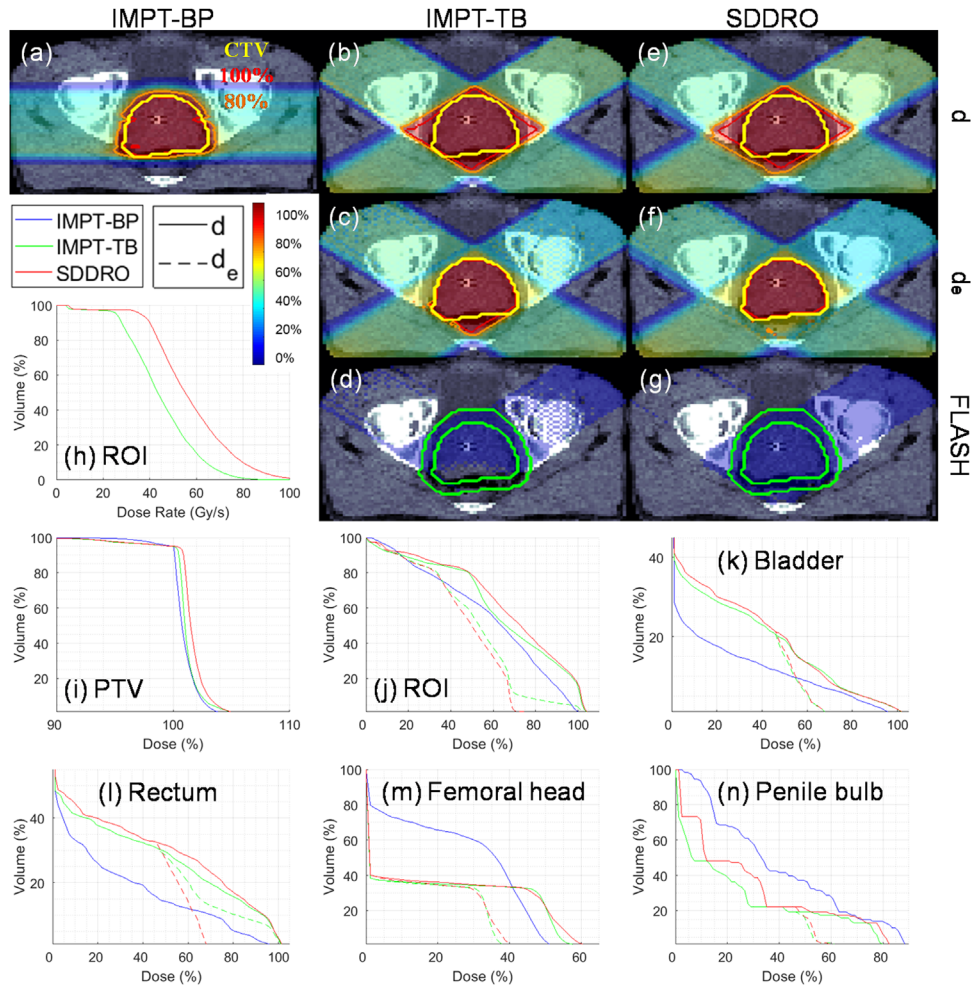


**FIGURE 2** Prostate. IMPT-BP: plot of dose in (a); IMPT-TB: plots of physical dose, FLASH effective dose, and FLASH coverage in (b)-(d); SDDRO: plots of physical dose, FLASH effective dose, and FLASH coverage in (e)-(g); DRVH for ROI in (h); DVH for PTV, ROI, bladder, rectum, femoral head, and penile bulb in (i)-(n). The dose plot window is [0%, 110%]. 100% isodose line, 80% isodose line, and PTV are highlighted in dose plots; ROI = PTV10mm is highlighted in FLASH coverage plots, in which the blanked region is without the FLASH effect

(Figures 1–4g), in which the colored region is with the FLASH effect, and the blanked region is without the FLASH effect. On the other hand, the dose rate volume histogram (DRVH) for ROI (Figures 1–4h) shows SDDRO improved FLASH dose rate coverage from IMPT-TB.

### 3.2 | Tradeoff between FLASH and dose optimization

Although the FLASH coverage was improved via SDDRO (see Section 3.1), the dose coverage was sacrificed to a certain extent. For example, for lung (Table 1), the CI decreased from 0.70 to 0.63, the mean physical dose of ROI increased from 26.6 Gy to 27.3 Gy, and the V20Gy of lung increased from 10.4cc to 11.2cc; this was also shown as an enlarged 80% isodose region in SDDRO (Figure 1e) compared to IMPT-TB (Figure 1b). Similar tradeoffs between FLASH and dose optimization

were also observed from other cases as shown in Table 1 and Figures 1–4. Note that this tradeoff is generic to FLASH, not specific to SDDRO, because maximization of the FLASH effect may have to increase the physical dose to meet the FLASH dose threshold (e.g.,  $d \geq 8\text{Gy}$ ).

### 3.3 | Resolving the tradeoff via FLASH effective dose

Given the tradeoff between FLASH and dose optimization, the physical dose  $d$  and the FLASH DMF were combined into FLASH effective dose  $d_e$ , with FLASH effective dose parameters summarized in Table 2 and FLASH effective dose plots in Figures 1–4. In light of the tradeoff, the results demonstrate that SDDRO improved the FLASH effective dose from IMPT-TB. For example, for lung, in terms of FLASH effective dose (Table 2), the CI increased from 0.85 to 0.95, the mean dose for

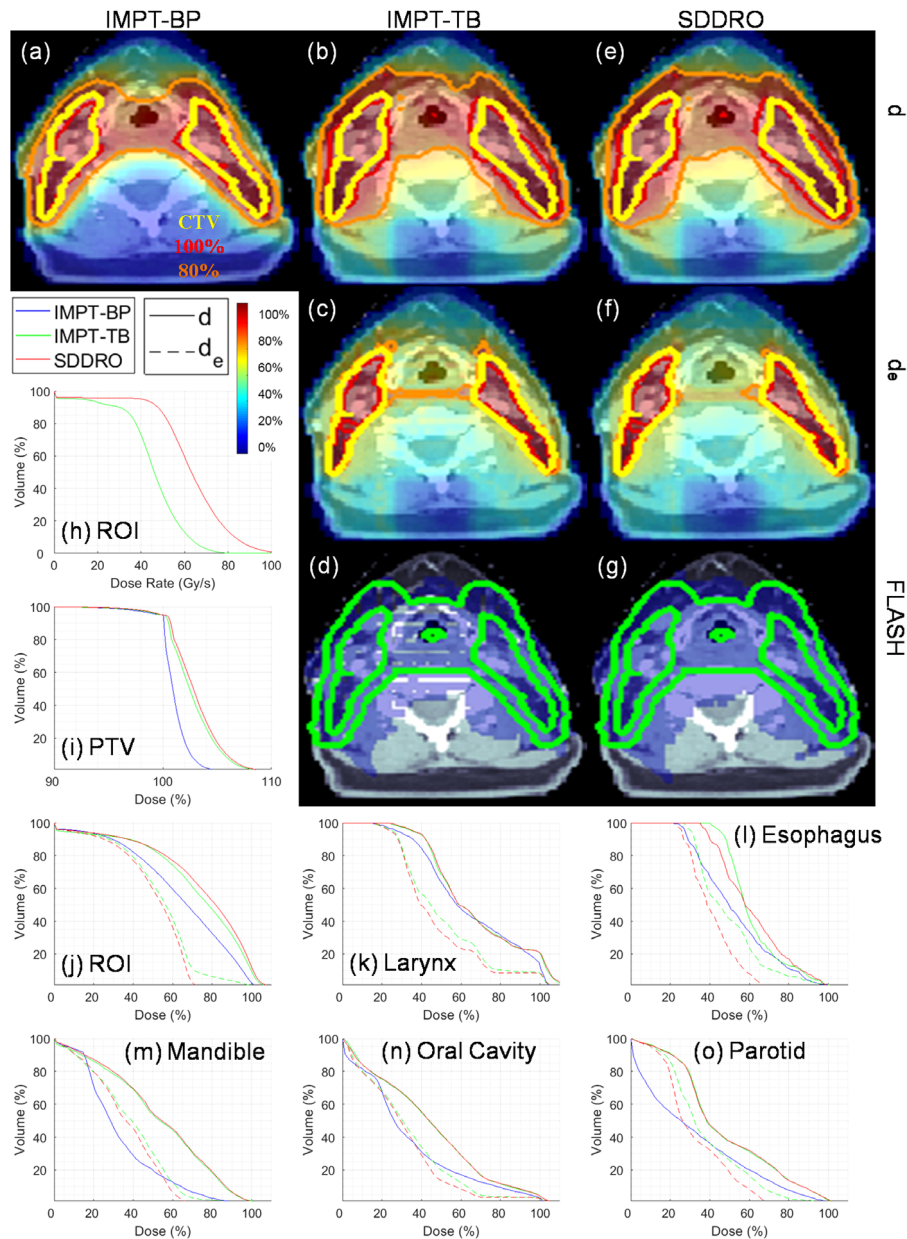


**FIGURE 3** HN. IMPT-BP: plot of dose in (a); IMPT-TB: plots of physical dose, FLASH effective dose, and FLASH coverage in (b)-(d); SDDRO: plots of physical dose, FLASH effective dose, and FLASH coverage in (e)-(g); DRVH for ROI in (h); DVH for PTV, ROI, larynx, esophagus, mandible, oral cavity, and parotid in (i)-(o). The dose plot window is [0%, 110%]. 100% isodose line, 80% isodose line, and PTV are highlighted in dose plots; ROI = PTV10mm is highlighted in FLASH coverage plots, in which the blank region is without the FLASH effect

the ROI decreased from 22.5 Gy to 19.9 Gy, and the V20Gy of lung decreased from 9.0cc to 8.0cc; SDDRO (Figure 1f) had a tighter 80% isodose region to the target than IMPT-TB (Figure 1c).

### 3.4 | Net effective change from CONV to FLASH

The results demonstrate that FLASH can spare more of high-dose OAR regions (e.g., ROI = PTV10mm) near treatment targets than CONV. In Table 2, the mean

FLASH effective doses of ROI from CONV (via IMPT-BP) to FLASH (via SDDRO) reduced from 23.7 Gy to 19.9 Gy for lung, from 20.8 Gy to 18.9 Gy for prostate, from 38.4 Gy to 30.8 Gy for HN, and from 8.6 Gy to 7.2 Gy for brain; these net effective changes were also demonstrated by DVH plots for ROI (Figure 1-4j), and the tighter 80% isodose region to the target by SDDRO (Figure 1f) than IMPT-BP (Figure 1a).

Noticeably, because of a reduced high dose near the target, FLASH can improve the target coverage from CONV. For example, in Table 2, the CI values increased from 0.89 to 0.95 for lung, and from 0.91 to 0.95 for HN,

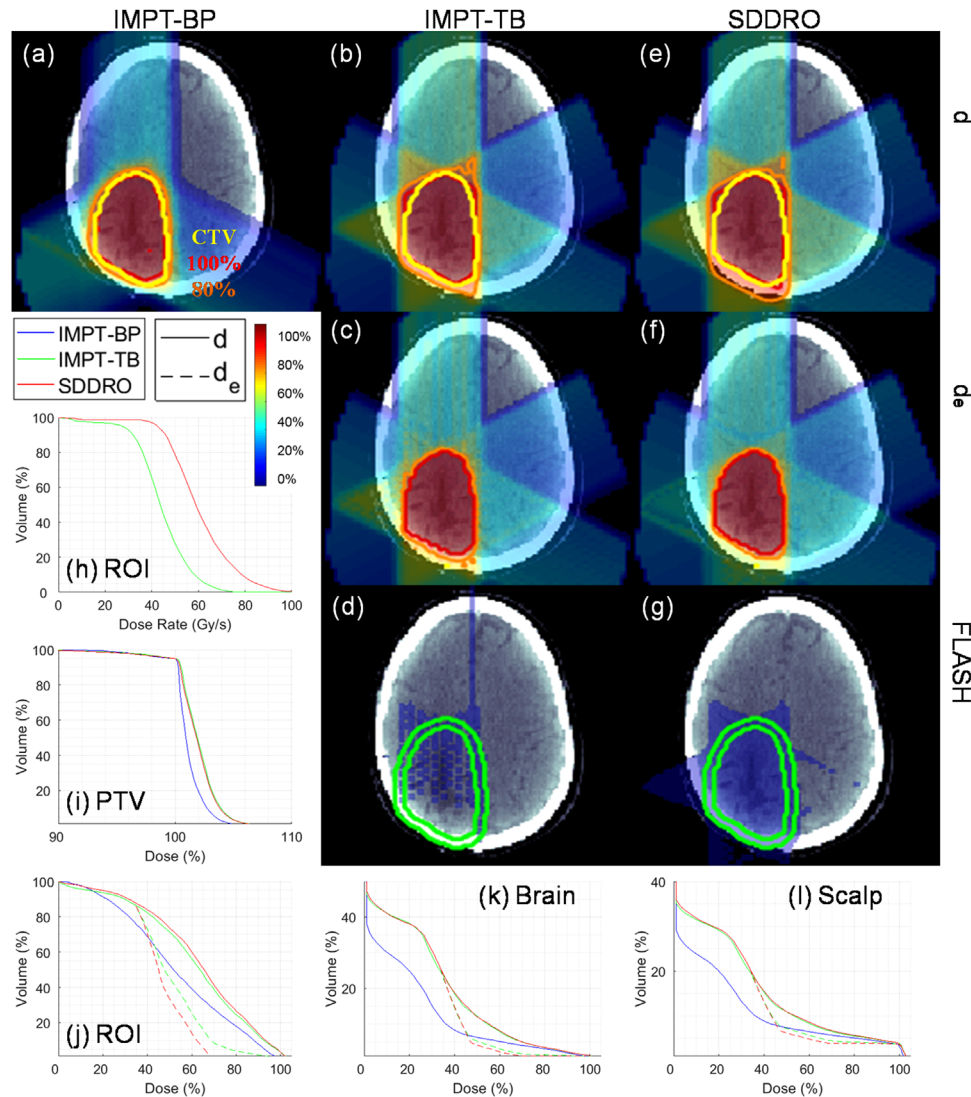


**FIGURE 4** Brain. IMPT-BP: plot of dose in (a); IMPT-TB: plots of physical dose, FLASH effective dose, and FLASH coverage in (b)-(d); SDDRO: plots of physical dose, FLASH effective dose, and FLASH coverage in (e)-(g); DRVH for ROI in (h); DVH for PTV, ROI, brain, and scalp in (i)-(l). The dose plot window is [0%, 110%]. 100% isodose line, 80% isodose line, and PTV are highlighted in dose plots; ROI = PTV10mm is highlighted in FLASH coverage plots, in which the blanked region is without the FLASH effect

from IMPT-BP to SDDRO. Note that  $CI = 0.95$  is optimal under the plan normalization  $D_{95\%} = 100\%$ .

### 3.5 | Meeting SBRT/SRS OAR constraints via SDDRO

The OAR planning constraints followed SBRT/SRS recommendations from recent HyTEC reports and others.<sup>40,42-44</sup> FLASH via SDDRO was able to meet some OAR constraints that CONV (IMPT-BP) failed to meet. For lung, per RTOG 0618,<sup>42</sup> the max dose constraint 27 Gy for esophagus was only met by FLASH via SDDRO (24.8 Gy), not CONV (35.3 Gy) or FLASH via IMPT-TB (36.6 Gy); the max dose constraint 30 Gy for trachea and bronchus was substantially relaxed to 22 Gy by SDDRO. For prostate, SDDRO substantially

decreased  $V_{32Gy}$  to nearly 0cc. For brain, compared to CONV, SDDRO substantially decreased  $V_{12Gy}$  from 43.9cc to 13.7cc; note that  $V_{12Gy} \leq 15cc$  is required to reduce the likelihood of symptomatic radiation necrosis per HyTEC reports.<sup>44</sup> All these improved high-dose sparing of OAR by FLASH via SDDRO may potentially enable proton SBRT/SRS that could otherwise fail to meet dose constraints by CONV, for example, the reduction of  $V_{12Gy}$  from 43.9cc to 13.7cc to meet  $V_{12Gy} \leq 15cc$  for this case to be eligible for brain SRS.

## 4 | DISCUSSION

We have shown that, compared to CONV-RT, FLASH-RT via SDDRO can provide not only better sparing for high-dose OAR (e.g., PTV10mm), but also better dose

**TABLE 1** Physical dose parameters

$d$	Structure	Quantity (Unit)	IMPT-BP	IMPT-TB	SDDRO
Lung	PTV	CI	0.89	0.70	0.63
	ROI	Dmean (Gy)	23.7	26.6	27.3
	Lung	V20Gy (%)	6.0	10.4	11.2
	Esophagus	Dmax (Gy)	35.3	37.1	37.2
	Trachea	Dmax (Gy)	30.4	31.9	32.4
	Bronchus	Dmax (Gy)	28.2	29.4	30.0
	Body	Dmean (Gy)	1.4	2.3	2.3
Prostate	PTV	CI	0.94	0.75	0.75
	ROI	Dmean (Gy)	20.8	23.9	25.2
	Bladder	V32Gy (cc)	5.4	8.4	8.3
	Rectum	V32Gy (cc)	5.2	19.2	20.3
	Body	Dmean (Gy)	1.2	2.2	2.3
HN	PTV	CI	0.91	0.77	0.74
	ROI	Dmean (Gy)	38.4	43.4	44.8
	Esophagus	Dmean (Gy)	31.6	37.0	36.8
	Larynx	Dmean (Gy)	38.6	40.2	40.4
	Mandible	Dmean (Gy)	20.0	31.6	32.2
	Cavity	Dmean (Gy)	20.3	26.5	26.6
	Parotid	Dmean (Gy)	19.3	28.6	28.6
	Body	Dmean (Gy)	3.7	5.5	5.8
Brain	PTV	CI	0.95	0.90	0.90
	ROI	Dmean (Gy)	8.6	9.9	10.2
	Brain	V12Gy (cc)	43.9	50.1	50.5
	Scalp	V12Gy (%)	5.4	6.0	6.1
	Body	Dmean (Gy)	0.7	1.0	1.0

**TABLE 2** FLASH effective dose parameters

$d_e$	Structure	Quantity (Unit)	IMPT-BP	IMPT-TB	SDDRO
Lung	PTV	CI	0.89	0.85	0.95
	ROI	Dmean (Gy)	23.7	22.5	19.9
	Lung	V20Gy (%)	6.0	9.0	8.0
	Esophagus	Dmax (Gy)	35.3	36.6	24.8
	Trachea	Dmax (Gy)	30.4	31.4	22.2
	Bronchus	Dmax (Gy)	28.2	29.4	22.1
	Body	Dmean (Gy)	1.4	2.2	2.1
Prostate	PTV	CI	0.94	0.92	0.95
	ROI	Dmean (Gy)	20.8	19.6	18.9
	Bladder	V32Gy (cc)	5.4	0.0	0.0
	Rectum	V32Gy (cc)	5.2	13.6	0.1
	Body	Dmean (Gy)	1.2	2.1	2.2
HN	PTV	CI	0.91	0.92	0.95
	ROI	Dmean (Gy)	38.4	32.3	30.8
	Esophagus	Dmean (Gy)	31.6	31.8	28.0
	Larynx	Dmean (Gy)	38.6	33.1	31.8
	Mandible	Dmean (Gy)	20.0	25.1	24.4
	Cavity	Dmean (Gy)	20.3	22.4	21.6
	Parotid	Dmean (Gy)	19.3	24.8	23.2
	Body	Dmean (Gy)	3.7	4.9	5.0
Brain	PTV	CI	0.95	0.94	0.95
	ROI	Dmean (Gy)	8.6	7.8	7.2
	Brain	V12Gy (cc)	43.9	18.4	13.7
	Scalp	V12Gy (%)	5.4	4.3	3.9
	Body	Dmean (Gy)	0.7	0.9	0.9

conformality to treatment target (e.g., CI), despite worse integral dose (e.g., the body mean dose in Tables 1 and 2). These promising FLASH results can be better appreciated, by realizing that FLASH-RT was planned with TB, which is usually suboptimal to BP (used for CONV-RT) for normal tissue sparing, since TB does not have the sharp dose falloff after exiting the target that can be achieved by BP. On the other hand, FLASH can be potentially achieved through other delivery mechanisms besides TB, such as TB based spread-out BP (SOBP) via ridge filters,<sup>25,27,45</sup> joint TB and BP,<sup>39</sup> and BP via proton LINAC with ultra-high dose rates for all energies,<sup>46</sup> for which SDDRO can be developed to optimize the FLASH effect. Although these delivery methods should offer better low-dose sparing of normal tissues similar to CONV-RT (e.g., the integral dose), TB is sufficient to demonstrate the unique benefit of FLASH-RT for sparing high-dose OAR, as shown in this study.

Different treatment planning and delivery methods need re-optimization of plan parameters. For example, the beam angles suitable for BP and TB are different (e.g., unlike BP, the opposing beams for TB provide

non-distinguishable dose influence matrices and thus are redundant), which can be solved for by beam angle optimization for a specific combination of treatment planning and delivery methods; spot distribution and weights after optimization are different (e.g., TB tends to have fewer spots with larger weights than BP; SDDRO tends to have higher minimum-MU g than IMPT-TB, and fewer spots with larger weights for a given g, owing to the dose rate optimization); the best weightings between plan objectives can also be different, since the inclusion of dose-rate or FLASH optimization and the use of TB instead of BP will change the Pareto surface from the multi-criteria optimization.

In current SDDRO formulation, the FLASH dose constraint and the FLASH dose rate constraint are enforced separately, i.e., the voxel meeting one constraint may not necessarily meet the other one. Given that the occurrence of the FLASH effect requires both dose and dose rate constraints, ideally these two constraints should be enforced jointly, that is, to maximize the volume meeting both constraints, and also to enforce neither constraints for the rest volume, for which the physical dose can

**TABLE 3** Dose-rate and FLASH coverage. Dose-rate coverage  $P_\gamma$ : The percentage of an OAR volume receiving  $\gamma \geq 40$  Gy/s; FLASH coverage  $P_{\gamma,d}$ : The percentage of an OAR volume receiving  $\gamma \geq 40$  Gy/s and  $d \geq 8$  Gy. Both  $P_\gamma$  and  $P_{\gamma,d}$  from IMPT-BP are zeros for all structures, and not individually listed in this table

$P_\gamma/P_{\gamma,d}$	Structure	IMPT-TB	SDDRO
Lung	ROI	48.7/37.2	96.5/67.1
	Lung	24.6/3.3	41.2/8.2
	Esophagus	18.4/2.2	32.8/4.1
	Trachea	38.0/16.6	58.9/24.6
	Bronchus	32.3/0.9	93.6/16.6
Prostate	ROI	59.0/39.1	90.8/58.4
	Bladder	33.3/10.4	36.8/11.3
	Rectum	13.2/7.2	39.8/24.4
HN	ROI	73.0/65.4	95.2/82.1
	Esophagus	64.3/37.9	100.0/61.1
	Larynx	84.0/51.9	100.0/63.0
	Mandible	77.2/42.6	94.5/51.1
	Cavity	80.3/31.0	95.8/37.6
	Parotid	56.4/24.6	92.0/35.5
Brain	ROI	65.3/50.8	97.0/73.3
	Brain	34.6/10.4	43.7/12.0
	Scalp	25.2/8.5	33.2/10.9

be better optimized. However, the joint requirement of two FLASH constraints becomes mathematically non-convex and may subsequently pose additional challenges for the optimizer. This will be investigated in the future.

Although the FLASH parameters (e.g.,  $\gamma_0$ ,  $d_0$ ,  $f$ ) used in this work are taken to be constants, the general framework of SDDRO Equation (1) and DMF model Equation (13) allows for heterogenous FLASH parameters. That is, the following can be modeled at no additional cost in terms of methodology and algorithm: (1) organ-dependent or voxel-based FLASH parameters and (2) multi-parametric FLASH parameters for a specific organ or voxel (i.e., via fitting ( $k_1$ ,  $k_2$ ) from multiple sets of ( $\gamma_0$ ,  $d_0$ ,  $f$ )).

On the other hand, instead of retrospective plan evaluation of FLASH effective dose via DMF, it is possible to incorporate DMF model into plan optimization and directly optimize FLASH effective dose for improved plan quality, which will be a future direction. Moreover, the evaluation or optimization of the overall effective dose can also include the linear energy transfer (LET).<sup>47–49</sup> However, LET is not considered in this study, because LET is not specific to FLASH, and the FLASH dose via TB has limited variation in LET.

The DADR is a mean dose rate. If needed, the instantaneous dose rate can also be regularized at voxels for each beamlet. Moreover, DADR does not account for spot scanning trajectory and beam-off time between

spots, which can be modeled by pencil beam scanning (PBS) dose rate.<sup>50</sup> In addition, the FLASH constraints do not account for the beam-off time between angle switching. Based on radiolytic oxygen depletion theory,<sup>11,15</sup> the oxygen level is sufficiently replenished after each beam switching (e.g., on the order of seconds). Therefore, the FLASH constraints can be regularized per beam angle instead, in which dose and dose-rate constraints for the FLASH effect are evaluated per field and FLASH effective doses are computed per field and then summed together for total FLASH effective dose. The current method is subject to these limitations, and we will investigate this in future work and update SDDRO with dose and dose rate constraints pertinent to the FLASH effect, to match the state-of-the-art understanding of FLASH mechanisms. Also note that the parameters and conclusions of this work based on DADR may subject to considerable changes for other forms of dose rate, for example, PBS dose rate.

The conclusions here are based on a specific set of FLASH parameters ( $\gamma_0 = 40$  Gy/s,  $d_0 = 8$  Gy,  $f = 0.7$  and  $k_1 = k_2 = 100$ ) and planning parameters (e.g., target dose per fraction). Without a detailed sensitive analysis for these parameters, we remark that the effective gain from CONV to FLASH should be enhanced for smaller dose rate threshold  $\gamma_0$ , smaller dose threshold  $d_0$ , smaller  $f$ , smaller  $k_1$  and  $k_2$ , and larger target doses per fraction.

The availability of SBRT/SRS is often hindered by dose-limiting toxicities to OAR. We demonstrated that compared to CONV-RT, FLASH-RT via SDDRO can substantially relax the high-dose constraints (e.g.,  $D_{max}$ ) for OAR close to the target (see Section 3.5), and therefore could be clinically significant in the sense that it may enable SBRT/SRS that are not allowed by CONV-RT due to the violation of critical dose constraints for OAR.

## 5 | FUTURE OUTLOOK

The contribution of SDDRO is to optimize the dose and dose-rate parameters associated with the FLASH effect, which IMPT do not explicitly optimize. However, SDDRO in its current form may not generate the desirable FLASH plan with maximized FLASH effect, for which we have the following future outlooks.

1. Modeling of state-of-the-art understanding of the FLASH effect. Although the exact mechanism and parameters that define the FLASH effect in humans are unknown, it may not prevent us from treating patients with FLASH, given the success of radiotherapy (RT) despite that we still do not have the exact answers to many fundamental RT questions (e.g., the exact mechanism and parameters for defining spatially-fractionated RT or linear energy transfer, or even the basic question how RT works). However, the

FLASH optimizer should keep up with the state-of-the-art understanding of the FLASH effect, e.g., a quantitative FLASH model,<sup>51</sup> and incorporate these FLASH models into the optimizer.

2. Optimization with respect to FLASH effective dose. Given the tradeoff nature between physical dose coverage and FLASH coverage, it is imperative to develop the optimization method that directly optimizes FLASH effective dose, which accounts for both physical dose and FLASH DMF. The modeling of DMF can be based on a simple step or sigmoid functions, or more complex spatiotemporal models (e.g., via radiolytic oxygen depletion<sup>11</sup>). Moreover, the availability of this optimizer can also enable the testing and optimizing of FLASH models and parameters via in-vivo studies.
3. Need of new optimization algorithms. The optimization of the FLASH effect is technically demanding, as it may involve spatiotemporal optimization of multi-scale (instantaneous or mean) dose and dose rate. For example, the optimization of PBS pattern (which is a combinatorial optimization problem) should be important to optimize the PBS dose rate (which is also a nonlinear optimization problem itself)<sup>50</sup>; the optimization of plan quality with large minimum-MU threshold  $g$  (for achieving ultrahigh dose rate) is a highly nonconvex problem. All these nonconvex and nonlinear optimization problems from FLASH present technical challenges, which may also be new to the optimization community.

## 6 | CONCLUSION

We have developed a new FLASH-RT plan optimization method via SDDRO that can account for both FLASH dose and dose rate constraints, and jointly optimize the FLASH effect and physical dose distribution. As a post-optimization evaluation tool, the FLASH effective dose that combines physical dose and FLASH DMF model has been proposed to resolve the generic trade-off between optimization of the FLASH effect and optimization of physical dose for normal tissues, and quantify the net effective change from CONV-RT to FLASH-RT. The FLASH effective dose results clearly show that FLASH-RT via SDDRO can improve the high-dose sparing of OAR from CONV-RT.

### ACKNOWLEDGMENT

The authors are very thankful to the valuable comments from anonymous reviewers. This research is supported in part by the NIH Grant No. R37CA250921.

### CONFLICT OF INTEREST

The authors have declared no conflict of interest.

## DATA AVAILABILITY STATEMENT

Research data are not shared.

## REFERENCES

1. Bourhis J, Montay-Gruel P, Jorge PG, et al. Clinical translation of FLASH radiotherapy: why and how?. *Radiother Oncol.* 2019;139:11-17.
2. Favaudon V, Caplier L, Monceau V, et al. Ultrahigh dose-rate FLASH irradiation increases the differential response between normal and tumor tissue in mice. *Sci Transl Med.* 2014;6:245ra293.
3. Montay-Gruel P, Petersson K, Jaccard M, et al. Irradiation in a flash: unique sparing of memory in mice after whole brain irradiation with dose rates above 100Gy/s. *Radiother Oncol.* 2017;124:365-369.
4. Loo BW, Schuler E, Lartey FM, et al. Delivery of ultra-rapid flash radiation therapy and demonstration of normal tissue sparing after abdominal irradiation of mice. *Int J Radiat Oncol Biol Phys.* 2017;98:E16.
5. Montay-Gruel P, Bouchet A, Jaccard M, et al. X-rays can trigger the FLASH effect: ultra-high dose-rate synchrotron light source prevents normal brain injury after whole brain irradiation in mice. *Radiother Oncol.* 2018;129:582-588.
6. Vozenin MC, De Fornel P, Petersson K, et al. The advantage of FLASH radiotherapy confirmed in mini-pig and cat-cancer patients. *Clin Cancer Res.* 2019;25:35-42.
7. Montay-Gruel P, Acharya MM, Petersson K, et al. Long-term neurocognitive benefits of FLASH radiotherapy driven by reduced reactive oxygen species. *Proc Natl Acad Sci.* 2019;116:10943-10951.
8. Vozenin MC, Hendry JH, Limoli CL. Biological benefits of ultrahigh dose rate FLASH radiotherapy: sleeping beauty awoken. *Clin Oncol.* 2019;31:407-415.
9. Fouillade C, Curras-Alonso S, Giuranno L, et al. FLASH irradiation spares lung progenitor cells and limits the incidence of radio-induced senescence. *Clin Cancer Res.* 2020;26:1497-1506.
10. Bourhis J, Sozzi WJ, Jorge PG, et al. Treatment of a first patient with FLASH-radiotherapy. *Radiother Oncol.* 2019;139:18-22.
11. Prax G, Kapp DS. A computational model of radiolytic oxygen depletion during FLASH irradiation and its effect on the oxygen enhancement ratio. *Phys Med Biol.* 2019;64:185005.
12. Smyth LML, Donoghue JF, Ventura JA, et al. Comparative toxicity of synchrotron and conventional radiation therapy based on total and partial body irradiation in a murine model. *Sci Rep.* 2018;8:12044.
13. Durante M, Bräuer-Krisch E, Hill M. Faster and safer? FLASH ultra-high dose rate in radiotherapy. *Br J Radiol.* 2018;91:20170628.
14. Labarbe R, Hotoiu L, Barbier J, et al. A physicochemical model of reaction kinetics supports peroxy radical recombination as the main determinant of the FLASH effect. *Radiother Oncol.* 2020;153:303-310.
15. Khan S, Bassenne M, Wang J, et al. Multicellular spheroids as in vitro models of oxygen depletion during FLASH irradiation. *Int J Radiat Oncol Biol Phys.* 2021;110:833-844.
16. Wilson JD, Hammond EM, Higgins GS, et al. Ultra-high dose rate (FLASH) radiotherapy: silver bullet or fool's gold?. *Front Oncol.* 2020;9:1563.
17. Kim MM, Darafsheh A, Schuemann J, et al., Development of Ultra-High Dose Rate (FLASH) Particle Therapy. *IEEE Transactions on Radiation and Plasma Medical Sciences.* 2021. <https://doi.org/10.1109/TRPMS.2021.3091406>.
18. Diffenderfer ES, Verginadis II, Kim MM, et al. Design, implementation, and in vivo validation of a novel proton FLASH radiation therapy system. *Int J Radiat Oncol Biol Phys.* 2020;106:440-448.

19. Buonanno M, Grilj V, Brenner DJ, et al. Biological effects in normal cells exposed to FLASH dose rate protons. *Radiother Oncol*. 2019;139:51-55.
20. Rama N, Saha T, Shukla S, et al. Improved tumor control through t-cell infiltration modulated by ultra-high dose rate proton FLASH using a clinical pencil beam scanning proton system. *Int J Radiat Oncol Biol Phys*. 2019;105:S164-S165.
21. Girdhani S, Abel E, Katsis A, et al. FLASH: a novel paradigm changing tumor irradiation platform that enhances therapeutic ratio by reducing normal tissue toxicity and activating immune pathways. *Cancer Res*. 2019;79:LB-280.
22. Girdhani S, Abel E, Katsis A, et al., FLASH: A novel paradigm changing tumor irradiation platform that enhances therapeutic ratio by reducing normal tissue toxicity and activating immune pathways. AACR Annual Meeting. 2019.
23. Iwata H, Toshito T, Omachi C, et al. Scanning Proton FLASH Irradiation Using a Synchrotron Accelerator: effects on Cultured Cells and Differences by Irradiation Positions. *Int J Radiat Oncol Biol Phys*. 2020;108:e522.
24. Darafsheh A, Hao Y, Zwart T, et al. Feasibility of proton FLASH irradiation using a synchrocyclotron for preclinical studies. *Med Phys*. 2020;47:4348-4355.
25. Liu R, Charyyev S, Zhou J, et al., Feasibility of 3D Printed Ridge Filter to Enable SBRT FLASH Therapy Using Scanning Proton Beam. AAPM Annual Meeting. 2021.
26. Mascia A, Zhang Y, Lee E, et al., Commissioning a Fixed Field FLASH Pencil Beam Scanning Proton Therapy System in Support of the First In-Human Clinical Trial. AAPM Annual Meeting. 2021.
27. Kim M, Verginadis I, Haertter A, et al., FLASH Sparing of Normal Tissue in a Proton Spread Out Bragg Peak. AAPM Annual Meeting. 2021.
28. van de Water S, Safai S, Schippers JM, et al. Towards FLASH proton therapy: the impact of treatment planning and machine characteristics on achievable dose rates. *Acta Oncol*. 2019;58:1463-1469.
29. van Marlen P, Dahele M, Folkerts M, et al. Bringing FLASH to the clinic: treatment planning considerations for ultrahigh dose-rate proton beams. *Int J Radiat Oncol Biol Phys*. 2020;106:621-629.
30. Gao H, Lin B, Lin Y, et al. Simultaneous dose and dose rate optimization (SDDRO) for FLASH proton therapy. *Med Phys*. 2020;47:6388-6395.
31. Breedveld S, Craft DL, Van Haveren R, et al. Multi-criteria optimisation and decision-making in radiotherapy. *Eur J Oper Res*. 2019;277:1-19.
32. Gao H, Clasié BM, McDonald M, et al. Plan-delivery-time constrained inverse optimization method with minimum-MU-per-energy-layer (MMPEL) for efficient pencil beam scanning proton therapy. *Med Phys*. 2020;47:3892-3897.
33. Boyd S, Parikh N, Chu E, et al. Distributed optimization and statistical learning via the alternating direction method of multipliers. *Foundations and Trends® in Machine learning*. 2011;3:1-122.
34. Goldstein T, Osher S. The split Bregman algorithm for l1 regularized problems. *SIAM J Imaging Sci*. 2009;2:323-343.
35. Gao H. Robust fluence map optimization via alternating direction method of multipliers with empirical parameter optimization. *Phys Med Biol*. 2016;61:2838-2850.
36. Lin Y, Clasié BM, Liu T, et al. Minimum-MU and sparse-energy-level (MMSEL) constrained inverse optimization method for efficiently deliverable PBS plans. *Phys Med Biol*. 2019;64:205001.
37. Gao H. Hybrid proton-photon inverse optimization with uniformity-regularized proton and photon target dose. *Phys Med Biol*. 2019;64:105003.
38. Gao H, Clasié BM, Liu T, et al. Minimum MU optimization (MMO): an inverse optimization approach for the PBS minimum MU constraint. *Phys Med Biol*. 2019;64:125022.
39. Lin Y, Lin B, Fu S, et al. SDDRO-Joint: simultaneous dose and dose rate optimization with the joint use of transmission beams and Bragg peaks for FLASH proton therapy. *Phys Med Biol*. 2021;66:125011.
40. Grimm J, Marks LB, Jackson A, et al. High Dose per Fraction, Hypofractionated Treatment Effects in the Clinic (HyTEC): an Overview. *Int J Radiat Oncol Biol Phys*. 2021;110:1-10.
41. Wieser HP, Cisternas E, Wahl N, et al. Development of the open-source dose calculation and optimization toolkit matRad. *Med Phys*. 2017;44:2556-2568.
42. RTOG-0618: A Phase II Trial of Stereotactic Body Radiation Therapy (SBRT) in the Treatment of Patients with Operable Stage I/II Non-Small Cell Lung Cancer.
43. Wang K, Mavroidis P, Royce TJ, et al. Prostate Stereotactic Body Radiation Therapy: an Overview of Toxicity and Dose Response. *Int J Radiat Oncol Biol Phys*. 2021;110:237-248.
44. Milano MT, Grimm J, Niemierko A, et al. Single- and multifraction stereotactic radiosurgery dose/volume tolerances of the brain. *Int J Radiat Oncol Biol Phys*. 2021;110:68-86.
45. Patriarca A, Fouillade C, Auger M, et al. Experimental set-up for FLASH proton irradiation of small animals using a clinical system. *Int J Radiat Oncol Biol Phys*. 2018;102:619-626.
46. Farr JB, Flanz JB, Gerbershagen A, et al. New horizons in particle therapy systems. *Med Phys*. 2018;45:e953-e983.
47. Paganetti H, ed. *Proton therapy physics*. CRC Press; 2016.
48. Giantsoudi D, Grassberger C, Craft D, et al. Linear energy transfer-guided optimization in intensity modulated proton therapy: feasibility study and clinical potential. *Int J Radiat Oncol Biol Phys*. 2013;87:216-222.
49. An Y, Shan J, Patel SH, et al. Robust intensity-modulated proton therapy to reduce high linear energy transfer in organs at risk. *Med Phys*. 2017;44:6138-6147.
50. Folkerts M, Abel E, Busold S, et al. A Framework for defining FLASH dose rate for pencil beam scanning. *Med Phys*. 2020;47:6396-6404.
51. Krieger M, van de Water S, Folkerts M, et al. A quantitative FLASH effectiveness model to reveal potentials and pitfalls of high dose rate proton therapy. *Med Phys*. 2021. XXXX.

**How to cite this article:** Gao H, Liu J, Lin Y, et al. Simultaneous dose and dose rate optimization (SDDRO) of the FLASH effect for pencil-beam-scanning proton therapy. *Med Phys*. 2021;1–12. <https://doi.org/10.1002/mp.15356>